An Independent Multichannel Imaging Research System for Ultrashort Echo Time Imaging on Clinical MR Systems

MARTYN N.J. PALEY,[1] EUGENY KRYUKOV,[1] MICHAEL LAMPERTH,[2] IAN R. YOUNG[3]

[1]*Academic Radiology, Department of Human Metabolism, University of Sheffield, Floor C, Royal Hallamshire Hospital, Sheffield S10 2JF, England*
[2]*Department of Mechanical Engineering, Imperial College, London SW7 2AZ, England*
[3]*Department of Electrical and Electronic Engineering, Imperial College, London SW7 2AZ, England*

ABSTRACT: Most clinical magnetic resonance systems do not have access to ultrashort echo time (UTE) imaging. The aim of this project was to develop a fully independent imaging insert for clinical MR systems to provide this new research application without disturbing routine operation. The initial clinical target for the system was improved orthopedic upper limb imaging using ultrashort repeat and echo time acquisitions. Echo times as short as TE = 80 μs were attained for standard 2DFT gradient echo sequences and TE = 25 μs for asymmetrically sampled radial acquisitions using the 160 mm inside diameter symmetrical cylindrical insert gradient set. The spectrometer was able to acquire 32 channels simultaneously with 14 bit resolution at up to 2.5 MS/s and had broadband operation from 250 kHz up to 200 MHz. Only eight active RF channels were constructed and used for this study. Acoustic noise with the insert coil was up to 30 dbA quieter than a whole body gradient system operating at the same gradient strength. The insert provides a useful method of performing UTE imaging using a standard clinical MRI system with no disturbance to normal operation. Concepts Magn Reson Part B (Magn Reson Engineering) 35B: 80–88, 2009

KEY WORDS: MRI; multichannel MR spectrometer; ultrashort echo time (UTE)

INTRODUCTION

Many clinical research systems do not have access to very short repeat or echo time sequences which are proving to be of great clinical interest (*1–20*). This is largely because of the constraints of whole body gradient systems which require very high pulsed power capability to generate sufficient gradient strength with consequent high levels of acoustic noise. The power required to produce a gradient field scales approximately as $G^2D^5/\Delta T$, where G is the gradient strength, D is a characteristic dimension for the coil, and ΔT is the risetime of the gradients. As the acquisition echo time tends toward zero, the gradient power requirement tends toward infinity. A practical way to get around this limitation is obviously to reduce the gradient coil dimensions, assuming that this is possible for the anatomy to be scanned. There are many possible methods to design MR gradient coils, and several groups have investigated insert coil sets capable of efficiently generating high-gradient strengths for a range of magnet geometries (*21–43*). However, these designs generally require use of the main system gradient drive amplifiers which requires a sophisticated switching unit potentially making the insert system less reliable. This could also possibly degrade performance of the clinical imaging system. A number of groups have also considered using

Received 14 January 2009; revised 21 February 2009; accepted 3 March 2009

Correspondence to: Martyn N.J. Paley; E-mail: m.n.paley@shef.ac.uk

Concepts in Magnetic Resonance Part B (Magnetic Resonance Engineering), Vol. 35B(2) 80–88 (2009)

Published online in Wiley InterScience (www.interscience.wiley.com). DOI 10.1002/cmr.b.20135

independent spectrometers to reduce these interfacing problems (*44–49*). This study aimed to create an independent imaging system including a multichannel spectrometer with gradient and RF coil inserts for imaging the upper limbs using very short echo times inside a whole body clinical MRI. Only the magnet was used from the clinical system, which meant that system hardware interactions were minimized. Images were acquired at 1.5T and 3T showing the flexibility of the insert system to enable research applications on clinical imagers.

The following specifications were set after discussions with a clinical advisory group:

1. The system would be located inside the imaging volume of a closed bore 1.5T or 3T MRI scanner, and should be independent of the scanner make and model.
2. The system should be capable of imaging or acquiring spectra from all biologically relevant nuclei in 1.5T or 3T magnets.
3. The system should be capable of acquiring data from up to 32 channels with ultrashort repeat times (<1 ms) and echo times (<100 μs).
4. The spectrometer system should be controlled by an intuitive graphical user interface.
5. The insert should not be affected by the magnetic field from the scanner.
6. The insert should produce acceptable acoustic noise (<90 dbA).
7. The system should be capable of switching between research and clinical modes within 5 min with absolutely no effect on the hardware or software of the clinical machine.
8. The insert should be light enough for a female technician to position on the patient table.

METHODS

Spectrometer and Software System

Control systems for MR systems often use proprietary digital signal processors which are programmed in low-level code and are difficult to upgrade when operating systems are inevitably changed to include new features. A recent trend in MR spectrometer design has been to include many receive and transmit channels to take advantage of parallel acquisition and transmission techniques. To make the spectrometer easier to upgrade with additional input and output channels as needed, it was decided to use industry standard data acquisition and control hardware and software. General purpose industrial control hardware and software has been created through thousands of man-years of effort by several large commercial companies to serve many and diverse industries and the spectrometer design could usefully take advantage of these extensive resources. A detailed review of available options was carried out based on company reputation, price, specification, and record for ongoing software support and hardware upgrade capability. Components were selected to match the input and output requirements for fast, parallel imaging in terms of numbers of channels and data throughput. The data acquisition system chosen was based on a PXI chassis with an embedded Windows XP controller which can acquire 32 channels simultaneously at 14 bit resolution at up to 2.5 MS/s (PXI6133, National Instruments, Austin, TX). Eight channels of 16 bit D-A conversion provided the control, RF and gradient waveforms at a maximum output rate of 1 MS/s (PXI 6733, National Instruments). The RF spectrometer used modular RF mixer (ZAD-3) and preamplifier (ZLF-500LN) components from Mini-Circuits (Brooklyn, NY). Only eight active RF channels were built because of cost constraints although the modular design could be easily extended to 32 channels to match the data acquisition system. The spectrometer used two 100 MHz synthesizers which were frequency doubled for operation at 3T (128 MHz) (PXI 5404, National Instruments). The frequency could be programmed from a few megahertz up to a maximum frequency of 200 MHz. This low-level control system was integrated with a 1.2 KW RF power amplifier (Tomco, Norwood, Australia) and 100 V, 92 A gradient drive amplifiers (Analogue Associates, Norwich, England) as shown in Fig. 1. A passive crossed diode TR switch was used to create very short switching time for the broadband radiofrequency power amplifier allowing ultrashort TR and TE operation as well as full multinuclear operation across a range of field strengths. A simplified schematic circuit diagram of the spectrometer is provided in Fig. 2.

Gradient Insert Coil

A number of methods have been previously used to design gradient coils including insert gradients for various magnet geometries (*21–43*). For this project, an insert gradient and RF coil system was required for upper limb orthopedic imaging. The internal diameter was set to 160 mm to allow imaging of the upper limb of a large adult male when used with an appropriate RF coil. This was then the basic dimension around which the three axis gradient coils were

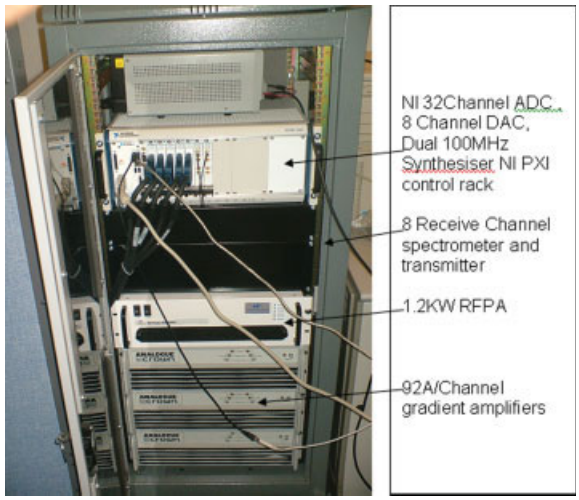

Figure 1 Photograph of the single cabinet independent MR spectrometer configuration. The spectrometer uses a single phase mains input (3KW) and can be sited in the main console room next to a waveguide. [Color figure can be viewed in the online issue, which is available at www.interscience.wiley.com.]

optimized. Because of the small diameter, the coil assembly was relatively distant from any conducting structures of the magnet assembly when localized at the iso-centre and so eddy current effects were predicted to be low. For this reason, it was decided not to shield the gradient set which results in much improved efficiency. To ensure as much as possible of the upper limb could be scanned, the overall gradient coil length was limited to 300 mm, thus constraining the design problem. A relatively conventional symmetrical design was chosen to ensure balanced forces. This was an important factor as the gradient set had to be held in place on a standard MR patient bed using standard Velcro strapping. For these reasons, a shortened, distributed "Maxwell pair" was chosen for the z-axis and shortened, distributed Golay coils for both the x- and y-axes. The trial coil set was modeled in 3D directly using the Biot–Savart law programmed in Matlab (Mathworks, Natick, MA). The locations of the main and return conductors were allowed to float independently within the coil former dimensional limitations and linearity along each axis was optimized using a least squares procedure. The mean spacing of the X, Y, and Z gradient coils from the optimization was 200 mm. The outer and inner turns of the X and Y saddles were at distances of 135 and 65 mm, respectively, from iso-centre and the minimum distance between active turns and the return paths was 40 mm. The geometry of the X and Y saddles is illustrated in Fig. 3(a). Figure 3(b) is a representative of 2D Biot–Savart simulation plot for the Y gradient set in an x-y plane offset from iso-centre by $+10$ mm. The X gradient was identical but rotated by 90°. Data from the Z gradient are not shown for brevity. The coils were wound with 30 turns of nonferromagnetic magnet wire (Comax Ltd., Upton, England) with a high temperature (180°C) polyester coating on the rigid 160 mm diameter, 300 mm length cylindrical former. The wire turns were secured in place and bound with fiber glass tape.

Gradient cables were fed through a waveguide and plugged into the gradient coils inside the screened room. The spectrometer was grounded to the screened room to reduce external radiofrequency

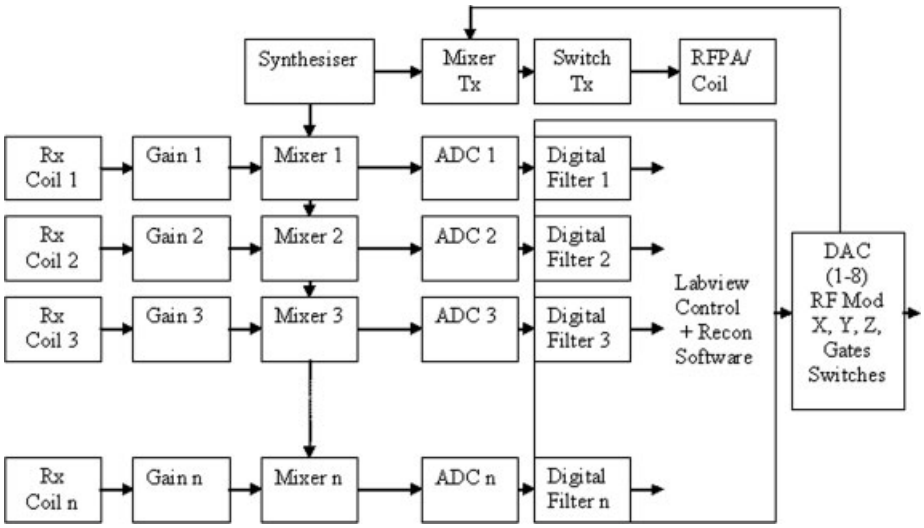

Figure 2 Schematic circuit diagram of the spectrometer and insert system.

interference. The inserts were tested on both 1.5T and 3T MR systems (Eclipse and Intera, respectively, Philips, Best, Netherlands) with conventional 75 and 100 mm circular transmit-receive (T/R) surface coils or a 100-mm diameter birdcage coil tuned to the appropriate frequency and matched to 50 Ω using a network analyzer (HP, Austin, TX). The RF coils were located at the centre of the gradient coil. The entire assembly was secured in the magnet using large Velcro straps attached to the patient bed as provided by the MR system manufacturer. Figure 3(c) shows the assembled gradient coil with a birdcage RF coil in place inside a 3T MR system.

Ultrashort TR/TE Sequences

A hard-coded sequential phase order FLASH sequence with a minimum TR of 680 μs and TE of 180 μs was created which simultaneously acquired up to 32 channels of data for a 64 × 210 matrix image in 38.8 ms. To create an even shorter TR/TE acquisition (STREACQ) sequence, profiles for 64 phase encode steps were programmed into each waveform file with a total of 27,800 points per channel. Acquisition of 32 channels of 14 bit digitally demodulated quadrature data used an outbound data rate of 700 kHz for the eight output channels and an inbound data rate of 700 kHz for each of the 32 inbound channels. In addition to the short TR/TE sequences, an ultrashort echo time (UTE) radial sequence was also built with an echo time of 10 μs from the end of the 25 μs half RF pulse [Fig. 8(a)]. In addition to these UTE sequences, a range of normal clinical imaging sequences such as gradient echo, spin echo, and inversion recovery were produced to test the insert coil assembly performance.

RESULTS

Gradient Coil Evaluation

The resistances of the X, Y, and Z coils were 0.4, 0.4, and 0.2 Ω and the inductances of the X, Y, and Z coils were 840, 780, and 580 μH, respectively, as measured using an LCR component analyser (LCR40, Peak Electronics, Buxton, England). The coils had efficiencies of 2.3, 2.1, and 2.7 mT/m/A for X, Y, and Z, respectively, measured using a gaussmeter (Model GM05, Hirst Magnetics Instruments, Falmouth, England) and a DC current of 10 A applied to each coil from a DC Power supply (IPS1810H, IsoTech RS, Corby, England). These efficiencies allowed maximum possible gradient strengths of 211, 193, and 248 mT/m for X, Y, and Z, respectively, with the gradient amplifiers used here although typically the image sequences used in this study had lower gradient strengths, e.g., 30 mT/m. The maximum possible slew rates were ~100 mT/m/ms with the gradient amplifiers used here but sequence rise times were limited to restrict slew rates to within safety guidelines for in vivo imaging to avoid peripheral nerve stimulation. The figures of merit defined as efficiency × radius$^{2.5}$ × inductance$^{-0.5}$ were 0.21, 0.24, and 0.35 for X, Y, and Z, respectively. The coils had much reduced acoustic noise (~30 dbA reduction) compared with the whole body gradient set for an equivalent imaging sequence as measured using a microphone (SM58, Shure Inc., Niles, IL) and a digital oscilloscope (Model, 2426Tektronix, Beaverton, OR) at the open scan room door. The coil assembly was easily located on the patient bed by a single operator and held in position using Velcro strapping.

Imaging Performance Tests

A series of imaging tests were performed at 1.5T and 3T to evaluate the gradient insert and RF coils in terms of linearity, SNR, and UTE performance. The phantoms and volunteers had to be carefully aligned centrally within the coil otherwise image distortion was created due to the relatively short regions of linearity on each gradient axis. Figure 4 (top) shows an axial gradient echo image acquired at 3T using a 100 mm T/R birdcage coil from the small structured phantom pictured in Fig. 4 (bottom) showing good linearity in the central axial plane. Geometric distortion of up to 10% is observed at the ends of the phantom on the sagittal image in Fig. 4 (middle) acquired with a larger of FOV = 80 mm showing the limits of the useable imaging region. Susceptibility artifacts from air bubbles can also be seen which affect the image uniformity. The phantom had an overall diameter of 35 mm, length of 70 mm, and the resolution inserts were 2 mm cross-section. Figure 5 shows an MR image of a hand acquired at 1.5T using the insert gradient system with a 100-mm birdcage RF coil and a Gradient Echo sequence.

UTE Imaging Tests

Figure 6 (top) illustrates the UTE capability of the insert system with an image of an undiluted Gd-DTPA 10 mL, 20-mm diameter, 70-mm length refill tube which has a very short T2* at 3T. Figure 6 (middle) shows results from a longer echo time sequence with TE = 5 ms at 3T. The signal from the Gd-DTPA has completely decayed by TE = 5 ms because of its very short T2* but is clearly visualized

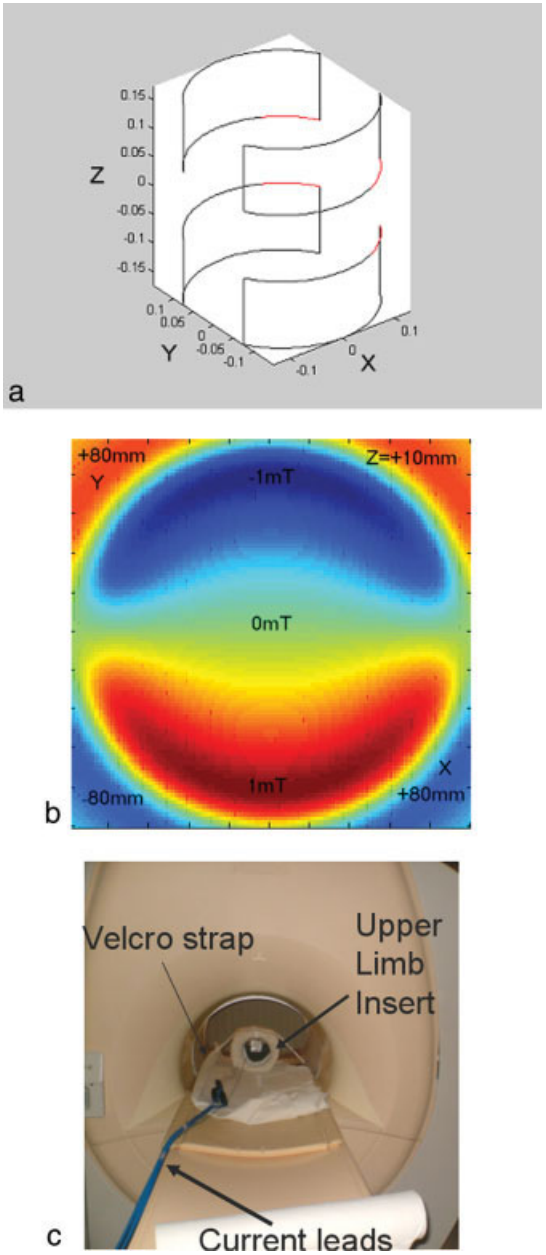

Figure 3 (a) 3D schematic plot of the mean coil positions for the distributed Golay X and Y gradient coils. Dimensions are in meters. (b) 2D plane from 3D Biot–Savart law simulation of the field from the upper limb Y gradient set located at $Z = +10$ mm. Similar simulations were performed for the X and Z coils. Nonlinearity was $<10\%$ within a 70 mm sphere located at the iso-centre of the coils for all three gradient axes. Data are normalized to ± 1 mT using the Matlab "color" scale. (c) Insert gradient set and RF coil located in the 3T MRI system. The blue cables feed current to the coils and the thin black cable is for the radiofrequency transmit-receive coil. The coil is held in place by a Velcro strap attached to the patient bed. [Color figure can be viewed in the online issue, which is available at www.interscience.wiley.com.]

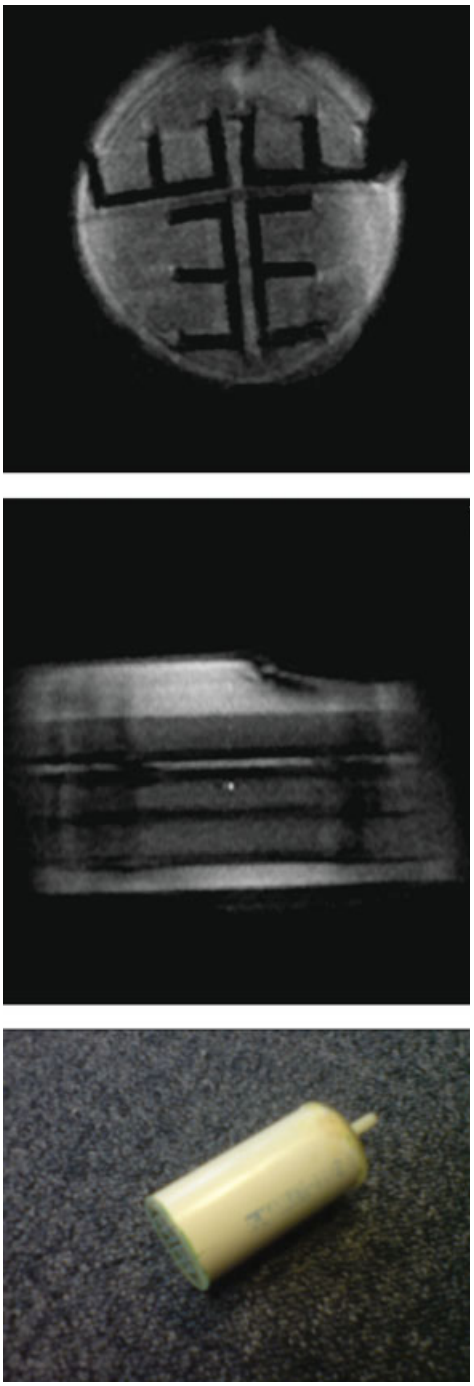

Figure 4 Top: Axial image acquired at 3T using a 100 mm diameter and length T/R birdcage coil with TR = 100 ms, TE = 4 ms, NEX = 4, SLT = 3 mm showing good linearity and high in-plane resolution of 500 μm × 250 μm. A sagittal image (middle) acquired at 3T with TR = 100 ms, TE = 4 ms, NEX = 4, in-plane resolution = 625 × 312 μm, SLT = 3mm shows up to 10% geometric distortion in the Z direction. The phantom (bottom) had an overall diameter of 35 mm and length of 70 mm. [Color figure can be viewed in the online issue, which is available at www.interscience.wiley.com.]

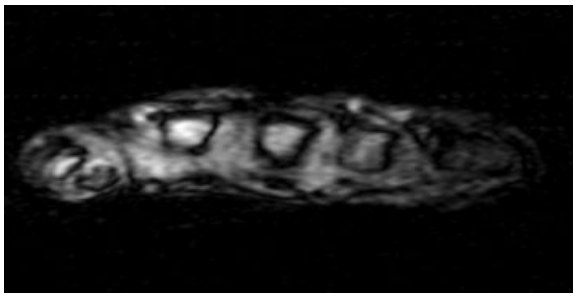

Figure 5 MR image of a hand acquired at 1.5T using the insert gradient system and 100 mm birdcage RF coil using a Gradient Echo sequence with TR = 500 ms, TE = 5 ms, NEX = 2, in-plane resolution = 1 mm × 0.5 mm, SLT = 5 mm.

at the short echo time allowed by the insert gradient set. The refill tube is pictured in Fig. 6 (bottom).

Figure 7 shows the central part of data set from the hard-coded STREACQ sequence described earlier showing the acquired MR echoes and the regular timing of the sequence despite the very short submillisecond repeat time of 680 μs at 3T. Figure 8(b) shows a radial image acquisition of a small 30 mL diameter vial of Gd-DTPA diluted 4:1with the sequence illustrated in Fig. 8(a) showing UTE imaging at 3T. The resolution was restricted because of the high-imaging acquisition bandwidth of 700 kHz used to minimize the echo time. The image was reconstructed using in-house Matlab code.

DISCUSSION AND CONCLUSION

The insert gradient set met its design requirements in terms of being low weight and easily installed or removed from the system within 5 min. This should make it a useful addition for research imaging on clinical scanners and could easily be used by a single MR technologist. The insert produced good quality images using both surface and birdcage coils at both 1.5T and 3T for conventional acquisitions. The useful region of gradient uniformity (10%) lay within a 70-mm sphere located at the centre of the coil which is adequate for high-resolution imaging of the upper extremity.

The UTE radial sequence achieved an ultrashort echo time of TE = 25 μs for radial scanning and TE = 80 μs for 2DFT scanning in conjunction with the gradient and RF coil insert which can switch rapidly. Gradient strengths up to 250 mT/m could be generated using the insert coil system although in this study the maximum was limited to more modest values typical of clinical imaging

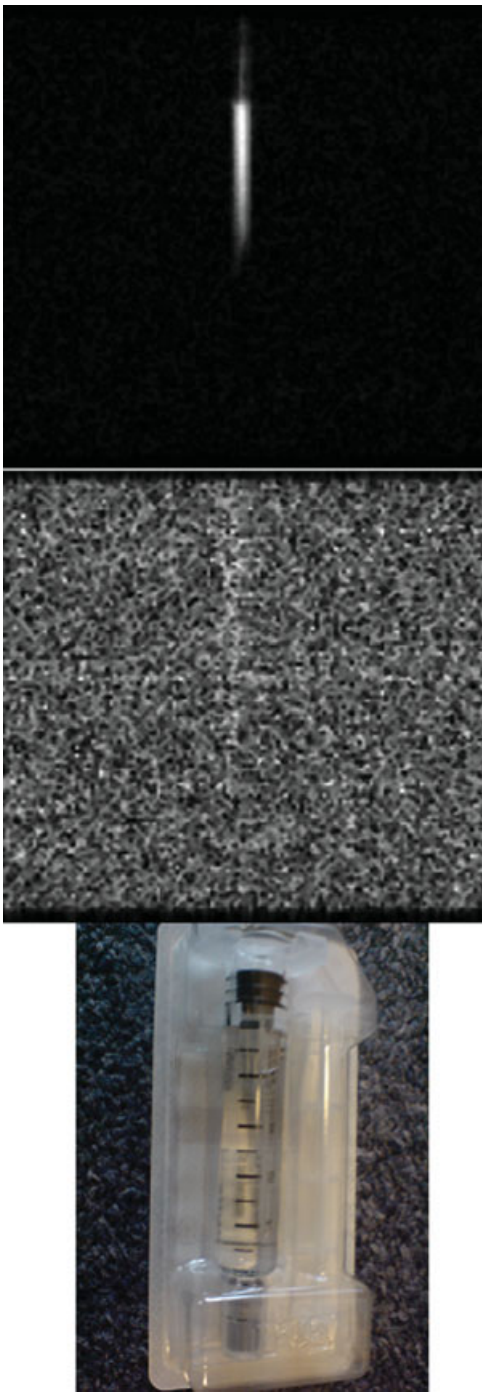

Figure 6 Top: Image of an undiluted Gd-DTPA 10 mL 20 mm diameter, 70 mm length refill tube which has a very short T2* acquired at 3T using TR = 70 ms, TE = 200 μs, NEX = 16, in-plane resolution = 1.2 mm × 0.6 mm, SLT = 2 mm. Image with same acquisition parameters (middle) except TE = 5 ms. The signal from the Gd-DTPA has completely decayed in the later echo time image. The refill tube is pictured (bottom). [Color figure can be viewed in the online issue, which is available at www.interscience.wiley.com.]

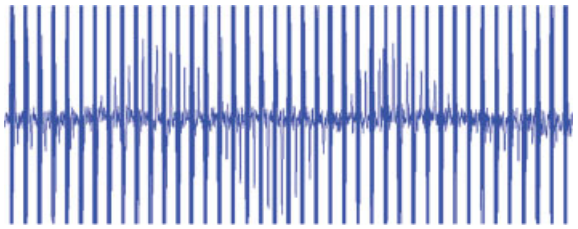

Figure 7 Central part of the k-space data set from a hard-coded ultrashort TR/TE acquisition (STREACQ) with TR = 680 μs, TE = 180 μs showing the regularly spaced MR echoes in between the RF pulses which are not blanked out during continuous acquisition of the entire 2D data set. [Color figure can be viewed in the online issue, which is available at www.interscience.wiley.com.]

systems due to mechanical constraints of the prototype coil. However, the acoustic noise was significantly quieter (~30 dbA) than the whole body gradients operating at the same gradient field strength. Also, the mechanical torque and associated vibrations from the coil were relatively low allowing easy location within the magnet and high resolution imaging. The slew rate with the 100 V amplifier used in this study was limited to 100 mT/m/ms which is still higher than most clinical MR systems which use significantly higher voltage gradient power supplies.

As the data acquisition hardware is modular and simultaneously samples each channel, the number of receive channels could be increased to at least 256 with no time penalty giving potential for a very sophisticated receive coil system. However, data handling and reconstruction of high-channel counts becomes a significant bottle neck with the single PC architecture used. Additional parallel PC's could be used to speed up the reconstruction process for very high-channel count systems. Alternatively, on the fly complex phased data addition could be used to speed up the reconstruction process by reducing the number of channels of data to reconstruct. In future, the STREACQ hard-coded ultrashort TR and TE sequence could be extended

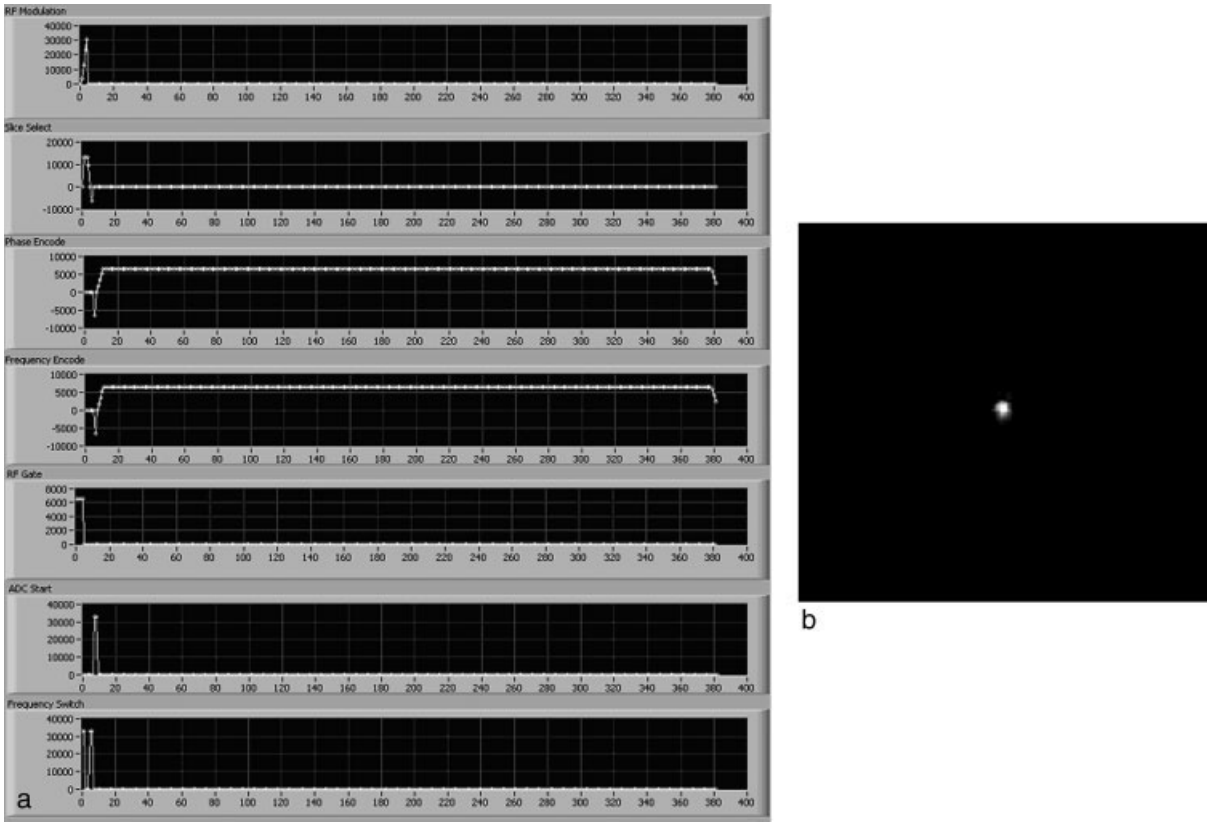

Figure 8 (a) Sequence diagram for ultrashort echo time radial imaging at 3T. (b) Axial image acquisition of a 30 mL vial of Gd-DTPA diluted 4:1 using TR = 500 ms, TE = 25 μs, NEX = 1, in-plane resolution = 4 mm × 2 mm, SLT = 5 mm showing ultrashort echo time imaging. The FOV was restricted because of the high-acquisition bandwidth of 700 kHz. The radial image was reconstructed using in-house Matlab code.

to a 3D acquisition by adding in a series of slice direction phase encode steps to allow ultrashort acquisition time 3D imaging potentially enabling subsecond volumetric imaging.

In summary, the lightweight gradient insert provides a range of additional capabilities for clinical MR scanners including high resolution and UTE imaging. Further work will investigate the clinical benefits of the insert system.

ACKNOWLEDGMENTS

This work was supported by UK Department of Health, New and Emerging Applications of Technology (NEAT, G019) and UK Department for Business, Enterprise and Regulatory Reform (BERR).

REFERENCES

1. Benjamin M, Milz S, Bydder GM. 2008 Magnetic resonance imaging of entheses. Part 1. Clin Radiol 63:691–703.
2. Benjamin M, Milz S, Bydder GM. 2008. Magnetic resonance imaging of entheses. Part 2. Clin Radiol 63:704–711.
3. Portman O, Flemming S, Cox JP, Johnston DG, Bydder GM. 2008. Magnetic resonance imaging of the normal pituitary gland using ultrashort TE (UTE) pulse sequences (REV 1.0). Neuroradiology 50:213–220.
4. Larson PE, Conolly SM, Pauly JM, Nishimura DG. 2007. Using adiabatic inversion pulses for long-T2 suppression in ultrashort echo time (UTE) imaging. Magn Reson Med 58:952–961.
5. Benjamin M, Bydder GM. 2007. Magnetic resonance imaging of entheses using ultrashort TE (UTE) pulse sequences (Review). J Magn Reson Imaging 25:381–389.
6. Tyler DJ, Robson MD, Henkelman RM, Young IR, Bydder GM. 2007. Magnetic resonance imaging with ultrashort TE (UTE) PULSE sequences: technical considerations (Review). J Magn Reson Imaging 25:279–289.
7. Robson MD, Bydder GM. 2006. Clinical ultrashort echo time imaging of bone and other connective tissues (Review). NMR Biomed 19:765–770.
8. Larson PE, Gurney PT, Nayak K, Gold GE, Pauly JM, Nishimura DG. 2006. Designing long-T2 suppression pulses for ultrashort echo time imaging. Magn Reson Med 56:94–103.
9. Rahmer J, Börnert P, Groen J, Bos C. 2006. Three-dimensional radial ultrashort echo-time imaging with T2 adapted sampling. Magn Reson Med 55:1075–1082.
10. Reichert IL, Robson MD, Gatehouse PD, He T, Chappell KE, Holmes J, et al. 2005. Magnetic resonance imaging of cortical bone with ultrashort TE pulse sequences. Magn Reson Imaging 23:611–618.
11. Gatehouse PD, Thomas RW, Robson MD, Hamilton G, Herlihy AH, Bydder GM. 2004. Magnetic resonance imaging of the knee with ultrashort TE pulse sequences. Magn Reson Imaging 22:1061–1067.
12. Gatehouse PD, He T, Puri BK, Thomas RD, Resnick D, Bydder GM. 2004. Contrast-enhanced MRI of the menisci of the knee using ultrashort echo time (UTE) pulse sequences: imaging of the red and white zones. Br J Radiol 77:641–647.
13. Robson MD, Benjamin M, Gishen P, Bydder GM. 2004. Magnetic resonance imaging of the Achilles tendon using ultrashort TE (UTE) pulse sequences. Clin Radiol 59:727–735.
14. Robson MD, Gatehouse PD, So PW, Bell JD, Bydder GM. 2004. Contrast enhancement of short T2 tissues using ultrashort TE (UTE) pulse sequences. Clin Radiol 59:720–726.
15. Robson MD, Gatehouse PD, Bydder GM, Neubauer S. 2004. Human imaging of phosphorus in cortical and trabecular bone in vivo. Magn Reson Med 51:888–892.
16. Hall-Craggs MA, Porter J, Gatehouse PD, Bydder GM. 2004. Ultrashort echo time (UTE) MRI of the spine in thalassaemia. Br J Radiol 77:104–110.
17. Chappell KE, Patel N, Gatehouse PD, Main J, Puri BK, Taylor-Robinson SD, et al. 2003. Magnetic resonance imaging of the liver with ultrashort TE (UTE) pulse sequences. J Magn Reson Imaging 18:709–713.
18. Robson MD, Gatehouse PD, Bydder M, Bydder GM. 2003. Magnetic resonance: an introduction to ultrashort TE (UTE) imaging (Review). J Comput Assist Tomogr 27:825–846.
19. Waldman A, Rees JH, Brock CS, Robson MD, Gatehouse PD, Bydder GM. 2003. MRI of the brain with ultra-short echo-time pulse sequences. Neuroradiology 45:887–892.
20. Gatehouse PD, Bydder GM. 2003. Magnetic resonance imaging of short T2 components in tissue (Review). Clin Radiol 58:1–19.
21. Turner R. 1993. Gradient coil design: a review of methods (Review). Magn Reson Imaging 11:903–920.
22. Mansfield P, Haywood B. 2008. Controlled E-field gradient coils for MRI. Phys Med Biol 53:1811–1827.
23. Haywood B, Chapman B, Mansfield P. 2007. Model gradient coil employing active acoustic control for MRI. MAGMA 20:223–231.
24. Aksel B, Marinelli L, Collick BD, von Morze C, Bottomley PA, Hardy CJ. 2007. Local planar gradients with order-of-magnitude strength and speed advantage. Magn Reson Med 58:134–143.
25. Wright AC, Bataille H, Ong HH, Wehrli SL, Song HK, Wehrli FW. 2007. Construction and calibration of a 50 T/m z-gradient coil for quantitative diffusion microimaging. J Magn Reson 186:17–25.
26. Green D, Leggett J, Bowtell R. 2005. Hemispherical gradient coils for magnetic resonance imaging. Magn Reson Med 54:656–668.

27. Mayer D, Zahr NM, Adalsteinsson E, Rutt B, Sullivan EV, Pfefferbaum A. 2007. In vivo fiber tracking in the rat brain on a clinical 3T MRI system using a high strength insert gradient coil. Neuroimage 35:1077–1085.
28. Mechefske CK, Wang F. 2006. Theoretical, numerical, and experimental modal analysis of a single-winding gradient coil insert cylinder. MAGMA 19:152–166.
29. Yao GZ, Mechefske CK, Rutt BK. 2004. Characterization of vibration and acoustic noise in a gradient-coil insert. MAGMA 17:12–27.
30. Tomasi D, Xavier RF, Foerster B, Panepucci H, Tannús A, Vidoto EL. 2002. Asymmetrical gradient coil for head imaging. Magn Reson Med 48:707–714.
31. Dodd SJ, Ho C. 2002. Short planar gradient coils for MR microscopy using concentric return paths. J Magn Reson 156:1–9.
32. Shvartsman SM, Brown RW, Cheng YC, Eagan TP, Fujita H, Morich MA, et al. 2001. Application of the SUSHI method to the design of gradient coils. Magn Reson Med 45:147–155.
33. Chronik BA, Alejski A, Rutt BK. 2000. Design and fabrication of a three-axis edge ROU head and neck gradient coil. Magn Reson Med 44:955–963.
34. Petropoulos LS. 2000. Finite size disc gradient coil set for open vertical field magnets. Magn Reson Imaging 18:615–624.
35. Chronik B, Alejski A, Rutt BK. 2000. Design and fabrication of a three-axis multilayer gradient coil for magnetic resonance microscopy of mice. MAGMA 10:131–146.
36. Liu H. An efficient geometric image distortion correction method for a biplanar planar gradient coil. 2000. MAGMA 10:75–79.
37. Crozier S, Roffmann WU, Luescher K, Snape-Jenkinson C, Forbes LK, Doddrell DM. 1999. An "openable," high-strength gradient set for orthopedic MRI. J Magn Reson 139:81–89.
38. Williams GB, Fisher BJ, Huang CL, Carpenter TA, Hall LD. 1999. Design of biplanar gradient coils for magnetic resonance imaging of the human torso and limbs. Magn Reson Imaging 17:739–754.
39. Caparelli EC, Tomasi D, Panepucci H. 1999. Shielded biplanar gradient coil design. J Magn Reson Imaging 9:725–731.
40. Bowtell R, Peters A. 1999. Analytic approach to the design of transverse gradient coils with co-axial return paths. Magn Reson Med 41:600–608.
41. Andrew ER, Kempka M. 1998. Transverse gradient coil with circle current paths. MAGMA 7:55–60.
42. Liu H, Truwit CL. 1998. True energy-minimal and finite-size biplanar gradient coil design for MRI. IEEE Trans Med Imaging 17:826–830.
43. Morvan D, Richard B, Fredy D. 1998. Experimental evaluation of nonlinearities of small-sized insertable gradient coils. Magn Reson Imaging 16:1257–1263.
44. Crozier S, Doddrell DM. 1998. A simple design methodology for elliptical cross-section, transverse, asymmetric, head gradient coils for MRI. IEEE Trans Biomed Eng 45:945–948.
45. Krjukov E, Fichele S, Wild JM, Paley MNJ. 2007. Design and evaluation of a low field system for hyperpolarized 3-He gas imaging of neonatal lungs. Concepts Magn Reson Part B: Magn Reson Eng 31B:209–217.
46. Liu Z, Zhao C, Zhou H, Feng H. 2006. A novel digital magnetic resonance imaging spectrometer. Conf Proc IEEE Eng Med Biol Soc 1:280–283.
47. Demas V, Herberg JL, Malba V, Bernhardt A, Evans L, Harvey C, et al. 2007. Portable, low-cost NMR with laser-lathe lithography produced microcoils. J Magn Reson 189:121–129.
48. Hoult DI, Kolansky G, Kripiakevich D. 2004. A 'Hi-Fi' Cartesian feedback spectrometer for precise quantitation and superior performance. J Magn Reson 171:57–63.
49. Paley M, Mayhew JE, Martindale AJ, McGinley J, Berwick J, Coffey P, et al. 2001. Design and initial evaluation of a low-cost 3-Tesla research system for combined optical and functional MR imaging with interventional capability. J Magn Reson Imaging 13:87–92.